NASA TECHNICAL NOTE

NASA TN D-4304

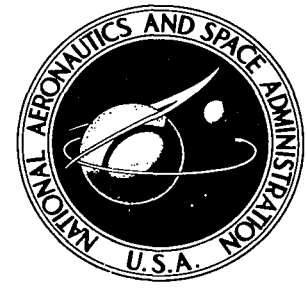

NASA TN D-4304

CALCULATIONS OF SOLAR PLASMA INTERACTION WITH MAGNETIC FIELD OF CURRENT LOOP AND TWO PARALLEL INFINITE LINES OF CURRENT

by Daniel J. McKinzie, Jr., and Anthony L. Julius, Jr.

Lewis Research Center
Cleveland, Ohio

NATIONAL AERONAUTICS AND SPACE ADMINISTRATION • WASHINGTON, D. C. • MARCH 1968

CALCULATIONS OF SOLAR PLASMA INTERACTION WITH MAGNETIC FIELD OF CURRENT LOOP AND TWO PARALLEL INFINITE LINES OF CURRENT

By Daniel J. McKinzie, Jr., and Anthony L. Julius, Jr.

Lewis Research Center
Cleveland, Ohio

NATIONAL AERONAUTICS AND SPACE ADMINISTRATION

For sale by the Clearinghouse for Federal Scientific and Technical Information
Springfield, Virginia 22151 – CFSTI price $3.00

CALCULATIONS OF SOLAR PLASMA INTERACTION WITH MAGNETIC FIELD OF CURRENT LOOP AND TWO PARALLEL INFINITE LINES OF CURRENT*

by Daniel J. McKinzie, Jr., and Anthony L. Julius, Jr.

Lewis Research Center

SUMMARY

An investigation was made of the forces resulting from the interaction of the unconfined magnetic field emanating from a space vehicle with the undisturbed solar plasma (solar wind). The integrated theoretical drag per unit area and the acceleration of a circular current loop exposed to the solar wind at zero degree angle of incidence were determined. Also, the integrated theoretical drag and lift per unit area, the restoring moment per unit area per unit length of span were determined for the case of two parallel infinite lines of current at a 45° angle of incidence. The calculations of these quantities were based on the theoretical results reported by Sprieter and Briggs (ref. 4).

For the case of the current loop, the drag per unit area varied from approximately 7.2×10^{-7} to 3.35×10^{-4} newton per square meter over a range of proton number densities from 10^{6} to 10^{8} particles per cubic meter and a magnetic field parameter from 10^{-4} to 10^{-2} tesla. An examination of the particle fluxes from a major solar flare showed it to have a negligible effect on the drag when compared with that from the solar wind. Accelerations were calculated for a hypothetical superconducting coil (hollow torus) that had a permanent unconfined magnetic field. The maximum acceleration calculated was approximately 1.37×10^{-4} meter per second squared. For the case of the two parallel infinite lines of current at a 45° angle of incidence, the lift to drag ratio was approximately 1 to 6.8.

INTRODUCTION

The discussion of the impact of a steady stream of plasma emanating from the Sun (solar wind) and interacting with the geomagnetic field of the Earth led Chapman and Ferraro (ref. 1) to the concept of a hollow volume (magnetosphere) carved out in space from which the solar wind is excluded. The magnetosphere (named by T. Gold) may be defined as the region in the vicinity of the Earth in which the Earth's magnetic field dom-

*Published in the Journal of Spacecrafts and Rockets, vol. 5, no. 1, 1968, pp. 3-8.

inates all particle dynamic processes. The boundary of the magnetosphere is called the magnetopause. In 1951 Martyn (ref. 2) described the steady plasma flow as exerting a constant pressure on the geomagnetic field whose own pressure maintains equilibrium. In 1958, Dungey (ref. 3) also pointed out that, for the case of steady-state conditions at the Earth's magnetopause, the aerodynamic pressure of the deflected stream is balanced by the magnetic and electrical forces on the charged particles.

Though the fundamental concept and equations governing the interaction between a neutral stream of ionized solar corpuscles and a three-dimensional magnetic dipole have been established for many years (ref. 4), the solution of the resulting equations has proved to be a difficult task. Most investigations of this problem have involved a reduction in the number of dimensions, but Beard (ref. 5) has presented an analysis in which the full three-dimensional character of the problem is retained throughout. He was able to derive a nonlinear partial differential equation for the coordinates of the magnetpause. However, Beard's results for the meridional plane did not satisfy the governing differential equation developed in the main body of the analysis. This fact was later pointed out by Sprieter and Briggs (ref. 4), and the problem was reworked for the meridional plane containing the dipole axis and the velocity vector of the incident stream for several cases in which these two directions were not perpendicular. The principal contribution of Sprieter and Briggs was the determination of the trace of the magnetospheric boundary in the meridional and equatorial planes for these several cases. The predicted profiles or limiting surfaces of the magnetosphere obtained in reference 4 are similar in scaled shape and size to the experimental results from reference 6 and also the satellite data of reference 7. The determination of the trace of the two dimensional magnetospheric boundary was also included in reference 4.

While the analysis of Sprieter and Briggs for the three-dimensional case is based on the assumption that the Earth's magnetic field may be approximated by the magnetic field of a dipole, the present analysis is based on the assumption that the magnetic field of a dipole may be approximated by the magnetic field of a current loop at large distances compared with the radius of the current loop. This assumption applies to the two-dimensional analysis also. It can be shown that, for the three-dimensional case (ref. 4), the maximum downstream cross-sectional area of the magnetosphere may vary from several to hundreds of times the projected area enclosed by the current loop, depending on the magnitude of its magnetic moment and the momentum of the plasma stream. Thus, the momentum exchange at the magnetopause produced by a current loop that is part of a space vehicle could have a significant effect on the motion of that vehicle. The possible magnitude of this effect is investigated in this report.

The theoretical analysis of reference 4 and its tabulated results are applied to determine the integrated momentum exchange over the magnetopause for two hypothetical space vehicle configurations. One configuration consists of a current loop (a three-

dimensional case), and the other consists of two parallel infinite lines of current (a two-dimensional case). The drag, lift, and moment are calculated for these cases. Finally, an estimate of the acceleration experienced by a nonlifting, hypothetical, hollow toroidal system is made. This system was studied for other purposes by Levy (ref. 8). All applications made in this report are for the condition that the relative velocity between the vehicle and the solar wind is equal to that of the solar wind with respect to the Sun.

SYMBOLS

A	area, m^2
a	radius of current loop for three-dimensional case, m
a_2	one-half normal separation distance for two-dimensional case, m
$\overline{B}$	total magnetic field vector, T
$\overline{B}_p$	permanent magnetic field vector, T
B_{po}	three-dimensional magnetic field parameter, T
$(B_{po})_2$	two-dimensional magnetic field parameter, T
B_s	total (tangential) magnetic field at magnetopause, T
$\overline{B}'$	induced magnetic field vector, T
b	unit length of span of two-dimensional magnetosphere (see fig. 3), m
c	speed of light, 3×10^8 m/sec
F	total lift or drag force (see fig. 6), N
F_D	total drag force (three dimensional), N
$(F_D)_2$	total drag force (two dimensional), N
$(F'_D)_2$	drag force (two dimensional) over upper magnetopause, N
$(F''_D)_2$	drag force (two dimensional) over lower magnetopause, N
$(F_L)_2$	total lift force (two dimensional), N
$(F'_L)_2$	lift force (two dimensional) over upper magnetopause, N
$(F''_L)_2$	lift force (two dimensional) over lower magnetopause, N
F_n	force (three dimensional) normal to magnetopause, N

$(F_n)_2$	force (two dimensional) normal to magnetopause, N
g	gravitational constant 9.814 m/sec^2
I	current, A
K	arbitrary constant of integration
M_2	total resultant moment acting about center of two-dimensional case (see fig. 4), N-m
$(M_D)_2$	total moment resulting from drag forces about center of two-dimensional case (see fig. 4), N-m
$(M_D)_{2(\varphi=\pi/2)}$	moment resulting from drag forces of two-dimensional case in $\varphi = \pi/2$ plane (see fig. 4), N-m
$(M_D)_{2(\varphi=-\pi/2)}$	moment resulting from drag forces of two-dimensional case in $\varphi = -\pi/2$ plane (see fig. 4), N-m
$(M_L)_2$	total moment resulting from lift forces acting about center of two-dimensional case (see fig. 4), N-m
$(M_L)_{2(\varphi=\pi/2)}$	moment resulting from lift forces of two-dimensional case in $\varphi = \pi/2$ (see fig. 4), N-m
$(M_L)_{2(\varphi=-\pi/2)}$	moment resulting from lift forces of two-dimensional case in $\varphi = -\pi/2$ plane (see fig. 4), N-m
M_p	magnetic moment of circular-current loop, $\pi a^2 I$, A-m^2
m	mass of positive ion (proton), 1.67×10^{-27} kg
n	number density of positive ions (protons) in undisturbed solar wind, particles/m^3
$\hat{n}_s$	unit vector in direction of outward normal to magnetopause
P_o	solar light pressure at Earth's orbit, 9×10^{-6} N/m^2
r	coordinate of permanent magnetic field and magnetopause, m
$\hat{r}$	unit radial vector
r_o	distance from apex of magnetosphere to center of three-dimensional current loop for special case in which $\lambda = 0$, m
$(r_o)_2$	distance from apex of magnetosphere to center of two parallel infinite lines of current for special case in which $\lambda = 0$, m
s	surface distance measured in meridional or equatorial plane, m
S_o	solar constant (eq. (47)) 1.35×10^3 J/(sec)(m^2)

s_o stagnation point in two- and three-dimensional cases, m

s_1 cutoff point of integration on three-dimensional magnetopause, where $|\cos \psi| \approx 0.03$ (see fig. 1), m

V velocity of positive ions (protons) in undisturbed solar wind relative to body considered, m/sec

$\overline{V}$ velocity vector, m/sec

θ coordinate of permanent magnetic field and magnetopause

θ_c cutoff point of integration

$(\theta_c)_B$ cutoff point of integration for lower magnetopause

$(\theta_c)_T$ cutoff point of integration for upper magnetopause

$\hat{\theta}$ unit meridional vector

θ_R $\theta - \lambda \sin \varphi$ (see fig. 4)

θ_s value of θ at pseudostagnation point (see figs. 3 and 4)

λ angle between direction of incident stream and plane of current system (angle of incidence)

λ_s $|\theta - \pi/2|$ (see figs. 3 and 4)

μ_o magnetic permeability in free space $4\pi \times 10^{-7}$ (kg)(m)/C^2

ρ dimensionless radial coordinate ($\rho = r/r_o$) of magnetopause

ρ_2 dimensionless radial coordinate $\left[\rho_2 = r/(r_o)_2\right]$ of magnetopause

φ coordinate of magnetopause (see fig. 2)

ψ angle between velocity vector of undisturbed particles of solar wind and outward normal to magnetopause at their point of impact (see fig. 1)

THEORETICAL CONSIDERATIONS

Presented herein are some of the more fundamental assumptions and equations on which the work of Sprieter and Briggs (ref. 4) is based. The assumptions are as follows: (1) A steady-state, neutral ionized corpuscular plasma stream flows radially outward from the Sun. (2) The geomagnetic field is represented by the field of a magnetic dipole. This magnetic field has the effect of creating a magnetosphere bounded by a thin current sheath (the magnetopause) that has the property of confining the solar plasma to

the exterior and the geomagnetic field to the interior of the magnetosphere. (3) Interior to the magnetopause

$$\nabla \times \overline{B} = 0$$

where $\overline{B}$ represents the magnetic field. (4) The particles of the solar stream move in straight lines to the magnetopause where they are, in effect, specularly reflected and and returned to the stream. In so doing, they exert an aerodynamic pressure of $2mnV^2 \cos^2\psi$ on any element of the boundary for which $\cos\psi \leq 0$, where ψ represents the angle between the velocity vector of the undisturbed particles of the solar wind and the outward unit normal vector $\hat{n}_s$ at the point of impact (see fig. 1) and m, n, and V represent the mass, number density, and velocity, respectively, of the positive ions relative to the body considered in the undisturbed solar wind. (Fig. 1 is a modification of a figure in ref. 4.) (5) An element of the surface that fails to comply with the condition that $\cos\psi \leq 0$ is shielded from the stream and experiences no aerodynamic pressure.

Dungey (ref. 3) showed that the aerodynamic pressure is balanced by the magnetic pressure $B_s^2/2\mu_o$, where B_s is the total (tangential) magnetic field in teslas, at the magnetopause. This pressure balance determines the location in space of the magnetopause. These considerations lead to the following relation that must be satisfied at the magnetopause.

$$\frac{B_s^2}{2\mu_o} = 2mnV^2 \cos^2\psi \tag{1}$$

(The equations developed in this report are written in the mks system of units.)

The total magnetic field $\overline{B}$ in the interior of the magnetosphere is the sum of the permanent magnetic field $\overline{B}_p$ and the induced magnetic field $\overline{B}'$ due to the currents in the magnetopause. As pointed out in reference 4, this field depends on the shape of the magnetopause, and its properties are described by the solution of the following magnetic-field equations

$$\text{div } \overline{B} = 0 \tag{2a}$$

$$\text{curl } \overline{B} = 0 \tag{2b}$$

which satisfy the boundary conditions that the normal component of $\overline{B}$ vanish and the tangential component of $\overline{B}$ be given by equation (1) at the magnetopause. For the three-

dimensional case (current loop), the permanent magnetic field where $r^2 >> a^2$ is given by

$$\overline{B}_p = -\frac{\mu_o M_p}{4\pi r^3}(\hat{\theta} \sin\theta + \hat{r}2 \cos\theta) \tag{3}$$

where M_p represents the magnetic moment of a circular current loop, a represents the radius of the current loop, I represents the current in the loop, r represents the radial coordinate of the permanent magnetic field, and $\hat{r}$ and $\hat{\theta}$ represent the unit coordinate vectors. In this report, B_{po} is defined as

$$B_{po} \equiv \frac{M_p \mu_o}{a^3 4\pi} \tag{4}$$

where B_{po} has units of magnetic field and is used as a parameter. As presented in reference 4, B_{po} is a measurable quantity (i.e., the magnetic field at the surface of the Earth), but herein, B_{po} as defined in equation (4), is simply a convenient parameter and does not necessarily specify the magnetic field at a or at any other specified point in space. Substituting into equation (3), yields

$$\overline{B}_p = -B_{po}\frac{a^3}{r^3}(\hat{\theta} \sin\theta + \hat{r}2 \cos\theta) \tag{5}$$

For the two-dimensional case,

$$\overline{B}_p = -\frac{\mu_o I}{\pi a_2}\frac{a_2^2}{r^2}(\hat{\theta} \sin\theta + \hat{r} \cos\theta) \tag{6}$$

where $2a_2$ represents the normal separation between the two parallel infinite lines of current, and where the condition $r^2 >> a_2^2$ must be satisfied. The magnetic field parameter for the two-dimensional case may be defined as

$$\left(B_{po}\right)_2 \equiv 4\left(\frac{\mu_o I}{4\pi a_2}\right) \tag{7}$$

where $\mu_o I/4\pi a_2$ is the magnetic field due to an infinitely long straight line of current

at a point of separation equal to $2a_2$. Substituting equation (7) into equation (6) results in

$$\bar{B}_p = - \left(B_{po}\right)_2 \frac{a_2^2}{r^2} (\hat{\theta} \sin \theta + \hat{r} \cos \theta) \tag{8}$$

It is assumed in reference 4 and in this report that the total tangential magnetic field at the magnetopause B_s is equal to twice the magnitude of $\bar{B}_p$ at the magnetopause. It should be noted that any magnetic system whose magnetic field may be expressed in either of the preceding forms (eqs. (5) or (8)) is similar to these systems.

In reference 4, the following differential equations were obtained for the location of the magnetopause in the meridional plane containing the dipole axis and the Sun-Earth line:

$$\frac{d\rho}{d\theta} = \rho \left\{ \frac{\rho^3 \sin[\theta - \lambda \sin(\pm\pi/2)] - \sin \theta}{\rho^3 \cos[\theta - \lambda \sin(\pm\pi/2)] + 2 \cos \theta} \right\} \tag{9}$$

and

$$\frac{d\rho}{d\theta} = \rho \left\{ \frac{\rho^3 \sin [\theta - \lambda \sin(\pm\pi/2)] + \sin \theta}{\rho^3 \cos[\theta - \lambda \sin(\pm\pi/2] - 2 \cos \theta} \right\} \tag{10}$$

These equations differ only in the signs of the last term in the numerator and denominator on their right sides. The solutions of these equations result in two families of curves that have been matched through physical reasoning to describe the complete profile of the magnetopause in the meridional plane. In equations (9) and (10), ρ is the dimensionless radial coordinate ($\rho = r/r_o$) of the magnetopause, λ represents the angle between the direction of the incident stream and the normal to the axis of the Earth, and θ is a spatial coordinate of the permanent magnetic field. The angle $\pm\pi/2$ represents the value of φ in the meridional plane (see fig. 2, a modification of a figure from ref. 4). The distance r_o is measured from the apex of the magnetosphere to the center of the dipole for the special case in which $\lambda = 0$. For the three-dimensional case (ref. 4),

$$r_o = \left[\frac{\mu_o M_p^2}{(4\pi)^2 mnV^2}\right]^{1/6} = a\left(\frac{B_{po}^2}{\mu_o mnV^2}\right)^{1/6} \tag{11}$$

The solutions of equations (9) and (10) are given by

$$\rho \cos[\theta - \lambda \sin(\pm\pi/2)] - \frac{1}{\rho^2} \cos\theta = K \tag{12}$$

and

$$\rho \cos[\theta - \lambda \sin(\pm\pi/2)] + \frac{1}{\rho^2} \cos\theta = K \tag{13}$$

where K is an arbitrary constant of integration. Only one solution from each family matches properly in the meridional plane to give the physically continuous profile shown in figure 1.

In reference 4, the final form of the differential equation for the shape of the magnetopause in the equatorial plane ($\theta = \pi/2$) is given. It is written for the special case where $\lambda = 0$ and φ is restricted to the interval $\pi/2 \leq \varphi \leq 3/2\ \pi$:

$$\frac{d\rho}{d\varphi} = \rho\left(\frac{\rho^6 \sin\varphi \cos\varphi + \sqrt{\rho^6 - 1}}{\rho^6 \cos^2\varphi - 1}\right) \tag{14}$$

The solution of this equation gives the shape of the magnetopause in the equatorial plane (fig. 2).

The foregoing is a presentation of some of the more fundamental assumptions and equations that made it possible for Sprieter and Briggs to describe the magnetopause of the Earth. They tabulated values representing the magnetopause as a function of θ and φ (see fig. 1). With the assumptions made herein that $r^2 >> a^2$ and $r^2 >> a_2^2$, the tabulated results of reference 4 are applicable to the cases of the current loop (three-dimensional case) and the two parallel infinite lines of current (two-dimensional case). The following is an analysis of the effect of the magnetic field solar wind interaction that gives rise to the forces over the magnetopause for the two- and three-dimensional cases.

Determination of Drag for Current Loop at Zero Angle of Incidence

If specular reflection is assumed at the magnetopause, the force normal to an element of area dA of the magnetopause can be written

$$dF_n = 2mnV^2(\cos^2\psi)dA \tag{15}$$

Now, from figure 1,

$$dA = 2\pi r_o^2(\cos\theta)\rho\, d\left(\frac{s}{r_o}\right) \tag{16}$$

where s is the distance along the surface and is measured in either the meridional, or the equatorial plane. The drag force acting in the direction of the velocity vector $\overline{V}$ is

$$dF_D = -(\cos\psi)dF_n \tag{17}$$

Substituting equations (15) and (16) into equation (17) and integrating yield

$$F_D = -4\pi mnV^2r_o^2 \int_{s_o/r_o}^{s_1/r_o} \cos^3\psi(\cos\theta)\rho\, d\left(\frac{s}{r_o}\right) \tag{18}$$

where s_1 is the cutoff point of integration on the magnetopause $|\cos\psi| \approx 0.03$ (see fig. 1), $(180 - \psi) \leq 90^\circ$, $\theta \leq 90^\circ$, and s_o represents the pseudostagnation point $s = 0$. In polar coordinates,

$$d\left(\frac{s}{r_o}\right) = \sqrt{\rho^2 + \left(\frac{d\rho}{d\theta}\right)^2}\, d\theta \tag{19}$$

When equation (19) is substituted into equation (18) and simplified, the results are

$$F_D = -4\pi mnV^2 r_o^2 \left(\left\{ \int_0^{\pi/2} \cos^3\psi(\cos\theta)\rho\left[\rho^2 + \left(\frac{d\rho}{d\theta}\right)^2\right]^{1/2} d\theta \right\}_{\varphi=\pi/2} + \left\{ \int_0^{\theta_c} \cos^3\psi(\cos\theta)\rho\left[\rho^2 + \left(\frac{d\rho}{d\theta}\right)^2\right]^{1/2} d\theta \right\}_{\varphi=-\pi/2} \right) \quad (20)$$

where the upper limit θ_c on the right side of equation (20) is the point at which the integrand becomes negligible and is the cutoff value $\theta_c = (5/12)\pi$ given in reference 4 (see fig. 1). The expression $\cos^3\psi$ may be written as an explicit function of θ. The first integral on the right side of equation (20) is the contribution to the drag in the plane $\varphi = \pi/2$ (fig. 1), while the second integral is the contribution in the plane $\varphi = -\pi/2$.

In deriving equation (20), the magnetopause was assumed to be axisymmetric. Figure 2 shows the shape of the magnetopause in the meridional and equatiorial planes. The figure indicates that the magnetopause is not axisymmetric, although the maximum downstream cross-sectional radius perpendicular to the y/a-axis appears to approach an asymptote of equal magnitude in both the equatorial and the meridional planes. Because of this asymmetry, two separate calculations were made by using the meridional-plane profile $\varphi = \pm 90^\circ$ in one case, and the equatorial plane profile $\theta = 90^\circ$ in the other. The agreement between the two values of the integrals, obtained by using the trapezodial rule, was within ±1 percent. The mean value of the resulting integral was -0.513. It is felt that there are no irregularities in the magnetopause in any other axial plane; thus, it is assumed that this value adequately represents the value of the integral. Substituting the mean value of the integral into equation (20), yields

$$F_D = 2.05\ mnV^2\pi r_o^2 \quad (21)$$

Determination of Lift and Drag for Two-Dimensional Case at 45° Angle of Incidence

Sprieter and Briggs (ref. 4) determined the differential equations that describe the trace of the magnetopause in the meridional plane for the two-dimensional case. The equations are

$$\frac{d\rho_2}{d\theta} = \rho_2 \left\{ \frac{\rho_2^2 \sin[\theta - \lambda \sin(\pm\pi/2)] - \sin\theta}{\rho_2^2 \sin[\theta - \lambda \sin(\pm\pi/2)] + \cos\theta} \right\} \tag{22}$$

and

$$\frac{d\rho_2}{d\theta} = \rho_2 \left\{ \frac{\rho_2^2 \sin[\theta - \lambda \sin(\pm\pi/2)] + \sin\theta}{\rho_2^2 \cos[\theta - \lambda \sin(\pm\pi/2)] - \cos\theta} \right\} \tag{23}$$

where ρ_2 is the dimensionless radial coordinate $\rho_2 = r/(r_o)_2$ of the magnetopause, and $(r_o)_2$ represents the distance from the apex of the magnetopause to the centerline between two parallel infinite lines of current for the special case in which $\lambda = 0$. From reference 4, the expression for $(r_o)_2$ is given by

$$(r_o)_2 = a_2 \left(\frac{B_{po}^2}{\mu_o mnV^2} \right)^{1/4} \tag{24}$$

The solutions of equations (22) and (23) are given by

$$\rho_2 \cos[\theta - \lambda \sin(\pm\pi/2)] - \frac{1}{\rho_2} \cos\theta = K \tag{25}$$

and

$$\rho_2 \cos[\theta - \lambda \sin(\pm\pi/2)] + \frac{1}{\rho_2} \cos\theta = K \tag{26}$$

where K is an arbitrary constant of integration. Sprieter and Briggs (ref. 4) solved these equations for the magnetopause of the two-dimensional case and tabulated values representing the magnetopause as a function of θ and ρ_2 in the meridional plane (see fig. 3). In the present analysis, only the tabulated values for $\lambda = 45^\circ$ were used because of the larger anticipated lift forces for this case. As in the three-dimensional case, the change in momentum over the magnetopause of the two-dimensional case that incorporates equation (19) is given by

$$d\left(F_n\right)_2 = 2mnb\left(r_o\right)_2 V^2 \cos^2\psi \left[\rho_2^2 + \left(\frac{d\rho_2}{d\theta}\right)^2\right]^{1/2} d\theta \tag{27}$$

where $\left(F_n\right)_2$ represents the local normal force acting on the differential area

$$\left(r_o\right)_2 b\left[\rho_2^2 + \left(\frac{d\rho_2}{d\theta}\right)^2\right]^{1/2} d\theta$$

of the surface of the magnetosphere, and b represents the length of the span of the two-dimensional magnetopause (see fig. 3).

Lift calculations. - The lift with respect to the wind axis (fig. 3) is given by

$$d\left(F_L\right)_2 = \sin\psi \, d\left(F_n\right)_2 \tag{28}$$

where the positive direction of the lift force is indicated in figure 3. Substituting equation (27) into equation (28) yields

$$d\left(F_L\right)_2 = 2mnb\left(r_o\right)_2 V^2 \cos^2\psi \sin\psi \left[\rho_2^2 + \left(\frac{d\rho_2}{d\theta}\right)^2\right]^{1/2} d\theta \tag{29}$$

where $\cos^2\psi$ and $\sin\psi$ are explicit functions of θ. Integrating equation (29) over the upper surface of the magnetopause shown in figure 3 results in

$$\left(F'_L\right)_2 = -2mnb\left(r_o\right)_2 V^2 \left(\left\{ \int_0^{\pi/2+\lambda_s} \cos^2\psi \sin\psi \left[\rho_2^2 + \left(\frac{d\rho_2}{d\theta}\right)^2\right]^{1/2} d\theta \right\}_{\varphi=\pi/2} + \left\{ \int_0^{\left(\theta_c\right)_T} \cos^2\psi \sin\psi \left[\rho_2^2 + \left(\frac{d\rho_2}{d\theta}\right)^2\right]^{1/2} d\theta \right\}_{\varphi=-\pi/2} \right) \tag{30}$$

where $\lambda_s = |\theta_s - \pi/2|$, and θ_s is the value of θ at the pseudostagnation point (fig. 3). The upper limit $(\theta_c)_T$ of the right side of equation (30) results in a negligible value of the integrand and is the cutoff value $(\theta_c)_T = \pi/6$ given in reference 4. Integrating equation (29) over the lower surface of the magnetopause yields

$$(F''_L)_2 = 2mnb(r_o)_2 V^2 \left(\left\{ \int_{\pi/2+\lambda_s}^{\pi} \cos^2\psi \sin\psi \left[\rho_2^2 + \left(\frac{d\rho_2}{d\theta} \right)^2 \right]^{1/2} d\theta \right\}_{\varphi=\pi/2} \right.$$

$$\left. + \left\{ \int_{(\theta_c)_B}^{\pi} \cos^2\psi \sin\psi \left[\rho_2^2 + \left(\frac{d\rho_2}{d\theta} \right)^2 \right]^{1/2} d\theta \right\}_{\varphi=-\pi/2} \right) \tag{31}$$

where the lower limit $(\theta_c)_B$ of the right side of equation (31) results in a negligible value of the integrand and is the cutoff value $(\theta_c)_B = \pi/3$ given in reference 4. Combining equations (30) and (31) yields

$$(F_L)_2 = (F'_L)_2 + (F''_L)_2 \tag{32}$$

which results in the total lift force over the two-dimensional magnetopause.

The evaluation of the integrals in equations (30) and (31) is 0.2897. Substituting this value into equation (32) results in

$$(F_L)_2 = 0.5794\ mnb(r_o)_2 V^2 \tag{33}$$

Drag calculations. - The drag, in the direction of the velocity vector $\overline{V}$ (fig. 3), is given by

$$d(F_D)_2 = -\cos\psi\ d(F_n)_2 \tag{34a}$$

where $d\left(F_n\right)_2$ is given by equation (27). Substituting equation (27) into equation (34a) and simplifying yield

$$d\left(F_D\right)_2 = -2mnb\left(r_o\right)_2 V^2 \cos^3\psi \left[\rho_2^2 + \left(\frac{d\rho_2}{d\theta}\right)^2\right]^{1/2} d\theta \tag{34b}$$

Integrating equation (34b) over the upper surface of the magnetopause (see fig. 3) results in

$$\left(F'_D\right)_2 = -2mn\left(r_o\right)_2 bV^2 \left(\left\{ \int_0^{\pi/2+\lambda} \cos^3\psi \left[\rho_2^2 + \left(\frac{d\rho_2}{d\theta}\right)^2\right]^{1/2} d\theta \right\}_{\varphi=\pi/2} + \left\{ \int_0^{\left(\theta_c\right)_T} \cos^3\psi \left[\rho_2^2 + \left(\frac{d\rho_2}{d\theta}\right)^2\right]^{1/2} d\theta \right\}_{\varphi=-\pi/2} \right) \tag{35}$$

where

$$\left(\theta_c\right)_T = \pi/6$$

For the lower surface

$$\left(F''_D\right)_2 = -2mn\left(r_o\right)_2 bV^2 \left(\left\{ \int_{\pi/2+\lambda}^{\pi} \cos^3\psi \left[\rho_2^2 + \left(\frac{d\rho_2}{d\theta}\right)^2\right]^{1/2} d\theta \right\}_{\varphi=\pi/2} + \left\{ \int_{\left(\theta_c\right)_B}^{\pi} \cos^3\psi \left[\rho_2^2 + \left(\frac{d\rho_2}{d\theta}\right)^2\right]^{1/2} d\theta \right\}_{\varphi=-\pi/2} \right) \tag{36}$$

where

$$\left(\theta_c\right)_B = \pi/3$$

Combining equations (35) and (36) results in

$$\left(F_D\right)_2 = \left(F'_D\right)_2 + \left(F''_D\right)_2 \tag{37}$$

which represents the total drag force over the two-dimensional magnetopause. The evaluation of the integrals in equations (35) and (36) is -1.976. Substituting this value into equation (37) results in

$$\left(F_D\right)_2 = 3.952\ mnb\left(r_o\right)_2 V^2 \tag{38}$$

Determination of Moment for Two-Dimensional Case at 45° Angle of Incidence

The moment about the axis of the two-dimensional case is illustrated in figure 4, which is a modification of a figure from reference 4. The assumption made in calculating this moment is that the two parallel infinite lines of current have been perturbed in such a manner that their angle of incidence is 45° to the velocity vector of the solar wind. In reference to figure 4, the moment resulting from the drag force is

$$\left(M_D\right)_2 = \left(M_D\right)_{2(\varphi=\pi/2)} + \left(M_D\right)_{2(\varphi=-\pi/2)} \tag{39}$$

Now, in the plane $\varphi = \pi/2$,

$$\left(M_D\right)_{2(\varphi=\pi/2)} = 2mn\left(r_o^2\right)_2 bV^2 \left\{ \int_0^{\pi} \rho_2 \cos\theta_R \cos^3\psi \left[\rho_2^2 + \left(\frac{d\rho_2}{d\theta} \right)^2 \right]^{1/2} d\theta \right\} \tag{40}$$

where

$$\theta_R = \theta - \lambda \sin \varphi$$

In the plane $\varphi = -\pi/2$,

$$\left(M_D\right)_{2(\varphi=-\pi/2)} = 2mn\left(r_o^2\right)_2 bV^2 \left\{ \int_0^{\left(\theta_c\right)_T} \rho_2 \cos\theta_R \cos^3\psi \left[\rho_2^2 + \left(\frac{d\rho_2}{d\theta}\right)^2\right]^{1/2} d\theta \right.$$

$$\left. + \int_{\left(\theta_c\right)_B}^{\pi} \rho_2 \cos\theta_R \cos^3\psi \left[\rho_2^2 + \left(\frac{d\rho_2}{d\theta}\right)^2\right]^{1/2} d\theta \right\} \qquad (41)$$

where $\left(\theta_c\right)_T = \pi/6$ and $\left(\theta_c\right)_B = \pi/3$.

The integrated moment resulting from lift forces is

$$\left(M_L\right)_2 = \left(M_L\right)_{2(\varphi=\pi/2)} + \left(M_L\right)_{2(\varphi=-\pi/2)} \qquad (42)$$

In the plane $\varphi = \pi/2$,

$$\left(M_L\right)_{2(\varphi=\pi/2)} = 2mn\left(r_0^2\right)_2 bV^2 \left\{ \int_0^{\pi/2+\lambda_s} \rho_2 \sin\theta_R \sin\psi \cos^2\psi \left[\rho_2^2 + \left(\frac{d\rho_2}{d\theta}\right)^2\right]^{1/2} d\theta \right.$$

$$\left. - \int_{\pi/2+\lambda_s}^{\pi} \rho_2 \sin\theta_R \sin\psi \cos^2\psi \left[\rho_2^2 + \left(\frac{d\rho_2}{d\theta}\right)^2\right]^{1/2} d\theta \right\} \qquad (43)$$

In the plane $\varphi = -\pi/2$,

$$\left(M_L\right)_{2(\varphi=-\pi/2)} = 2mn\left(r_o^2\right)_2 bV^2 \left\{ - \int_0^{\left(\theta_c\right)_T} \rho_2 \sin\theta \sin\psi \cos^2\psi \left[\rho_2^2 + \left(\frac{d\rho_2}{d\theta}\right)^2\right]^{1/2} \right.$$

$$\left. + \int_{\left(\theta_c\right)_B}^{\pi} \rho_2 \sin\theta_R \sin\psi \cos^2\psi \left[\rho_2^2 + \left(\frac{d\rho_2}{d\theta}\right)^2\right]^{1/2} d\theta \right\} \qquad (44)$$

where $\left(\theta_c\right)_T = \pi/6$ and $\left(\theta_c\right)_B = \pi/3$.
Therefore, the total resultant moment is given by

$$M_2 = \left(M_D\right)_2 + \left(M_L\right)_2 \qquad (45)$$

Because $2mnbV^2\left(r_o^2\right)_2$ is a common factor in equations (40) to (45), all the integrals may be summed. The value of their summation is approximately 0.066. The resultant moment acts as a restoring moment (fig. 4). Thus, the total moment evaluated for the two-dimensional case at a 45° angle of incidence to the solar wind is given by

$$M_2 \approx 0.1320\ mnb\left(r_o^2\right)_2 V^2 \qquad (46)$$

DISCUSSION OF RESULTS

The results of calculations made by using the preceding analyses are presented in figures 5 to 7. Figure 5 is a plot of the magnetic field parameter B_{po} against the ratio of the drag to a^2 for the current loop at a zero degree angle of incidence to the solar wind. The curves are plotted for a constant proton number density n of the solar wind. The number densities considered are 10^6, 10^7, and 10^8 particles per cubic meter. The number density is implicit in the relation between B_{po} and the drag per unit area. The data were computed by assuming the mean relative velocity of the undisturbed solar wind to be 5×10^5 meters per second. An examination of the effect of a major solar flare showed that it makes little or no contribution to the magnetic interaction forces because of its small particle flux densities. Also shown in figure 5 is the value of the ratio of the drag to a^2 that results from light pressure acting on a circular normally oriented re-

flective surface having a radius a equal to that of the current loop. The resulting drag was calculated by assuming the value of the solar light pressure at the Earth's obrit to be

$$P_o = \frac{2S_o}{c} = 9\times10^{-6}\ N/m^2 \tag{47}$$

where

$$S_o = 1.35\times10^{3}\ J/(sec)(m^2)$$

and

$$c = 3\times10^{8}\ m/sec$$

The ratio of the drag per unit area (due to the solar wind magnetic field interaction) to that of the solar light pressure varies from a minimum of approximately 2.5×10^{-2} to a maximum of approximately 12 over the range of the magnetic field and number density considered. Thus, if the magnetic moment of the current loop is large enough, the interaction of the solar wind with the magnetic field of the loop can result in a larger drag force than that due to solar light pressure.

In order to assess the navigational possibilities of the forces resulting from the interaction, a two-dimensional case was analyzed because of its mathematical simplicity. Calculations were made for a 45^{o} angle of incidence to the solar wind. These indicated that the two lines of current would experience a lift to drag ratio of approximately 1 to 6.8. The curves of lift and drag per unit area, respectively, are shown in figure 6 and are plotted against $(B_{po})_2$. The unit area referred to in this case is the unit length of span b multiplied by half the separation distance a_2 of the two infinite parallel lines of current (see fig. 3). As in the three-dimensional case, the curves are plotted for constant proton number density n. Because the lift and drag forces are a function of the size and shape of the magnetopause, a multiplicity of field sources could possibly be arranged to create various desirable shapes of the resultant magnetopause. The overall shape may range from a thin high-lift wedge to a blunt high-drag hemisphere.

The existence of lift and drag forces may imply a resultant moment. Figure 7 is a plot of $(B_{po})_2$ against the restoring moment per unit area per unit length of span b for the two-dimensional case. The unit area for this case is the square of one-half the separation distance between the two lines of current. In calculating this moment, it is assumed that the two parallel infinite lines of current have been perturbed in such a manner

that their angle of incidence is 45^{o} to the velocity vector of the solar wind. The curves are plotted for constant proton number density n. The existence of the restoring moment suggests that a method of attitude stabilization of this configuration with respect to the solar wind is available since a moment only exists for an angle of incidence greater than zero. It also implies that an additional force is necessary to overcome this restoring moment in order to utilize the lift in a navigational capacity.

To gain an idea of the magnitude of the accelerations that might be experienced, a hypothetical toroidal system was chosen. Estimates of the mass and the radius a of the toroid were based on the hypothetical hollow toroid system of reference 8. The system presented in reference 8 was devised to provide a toroidally shaped radiation-free volume. This volume would be shielded from solar and galactic corpuscular radiation having energies equal to and less than a specified value. In the present application, the system was designed to shield a volume of 10^5 cubic meters from proton energies of 200 MeV or less. The calculations were made by assuming a zero angle of incidence. The resulting mass, current, radius of the current loop, and magnetic field parameter were approximately 3×10^6 kilograms, 4×10^6 amperes, 3.3 kilometers, and 3.80×10^{-4} tesla, respectively.

The application of the analysis of the geomagnetic field interaction with the solar wind (ref. 4) to a vehicular system such as that of reference 8 is subject to the condition that similarity criteria be satisfied. These criteria are set forth in reference 9. Of concern in the simulation is the condition that no ring currents exist ($\nabla \times \overline{B} = 0$) within the magnetosphere of the hypothetical toroidal system, and also that the ion cyclotron radius of the protons at the magnetopause be less than the standoff distance of the magnetopause. The second, ion cyclotron radius, requirement is very important because it is at the magnetopause that the exchange of momentum from the solar wind takes place. These requirements have been satisfied in the calculation of the accelerations shown in table I:

TABLE I. - THEORETICAL ACCELERATIONS OF TOROIDAL SYSTEM

Three-dimensional magnetic field parameter, B_{po}, T	Density, n, protons/m^3	Acceleration of toroidal system[a]		Sunlight reflective acceleration system[b]	
		m/sec^2	g	m/sec^2	g
3.80×10^{-4}	5×10^6	1.85×10^{-5}	1.88×10^{-6}	3×10^{-3}	3.06×10^{-4}
3.80	10^7	2.95	3.01	3	3.06
3.80	10^8	1.37×10^{-4}	1.40×10^{-5}	3	3.06

[a]Ref. 8.
[b]Ref. 10.

The accelerations are compared with the acceleration presented in reference 10 which results from the reflection of sunlight at 1 astronomical unit by a sheet of material with a specific gravity of 1.18 and a thickness of approximately 7.61×10^{-6} meter. The area of the sheet is equal to that of a disk which has the same maximum radius as that of the toroidal system, and no mass has been included for the structural support of the sheet. The maximum calculated value of the acceleration of the hypothetical toroid considered is 1.37×10^{-4} meter per second squared ($\sim10^{-5}$ g). This value is $1\frac{1}{2}$ orders of magnitude lower than that experienced by the sheet in sunlight at 1 astronomical unit.

SUMMARY OF RESULTS

The results obtained from an investigation of the forces resulting from the interaction of a magnetic field possessed by a hypothetical space vehicle with solar wind are as follows:

1. The ratio of the drag due to the interaction of the magnetic field of a current loop with the undisturbed solar wind to solar light pressure drag imparted to a reflective surface that has an area equal to the area of the loop is approximately 2.5×10^{-2} to 12 over the range of proton number densities and magnetic field considered.

2. For the two-dimensional case at a 45° angle of incidence, the ratio of the lift to the drag is approximately 1 to 6.8 and a restoring moment exists.

3. The maximum calculated value of acceleration of the hypothetical toroid considered is 1.37×10^{-4} meter per second squared ($\sim10^{-5}$ g). This value is $1\frac{1}{2}$ orders of magnitude lower than that experienced in sunlight at 1 astronomical unit by a sheet of very light reflective material for which no structural supporting weight has been included.

Lewis Research Center,
National Aeronautics and Space Administration,
Cleveland, Ohio, February 3, 1967,
129-01-05-05-22.

REFERENCES

1. Chapman, S.; and Ferraro, V. C. A.: A New Theory of Magnetic Storms. Terr. Mag. & Atoms. Elec., vol. 36, June 1931, pp. 77-97; vol. 36, Sept. 1931, pp. 171-186; and vol. 37, June 1932, pp. 147-156, 421-429.

2. Martyn, D. F.: The Theory of Magnetic Storms and Auroras. Nature, vol. 167, Jan. 30, 1951, pp. 92-94.

3. Dungey, J. W.: Cosmic Electrondynamics. Cambridge University Press, 1958.

4. Spreiter, John R.; and Briggs, Benjamin R.: Theoretical Determination of the Form of the Hollow Produced in the Solar Corpuscular Stream by Interaction with the Magnetic Dipole Field of the Earth. NASA TR R-120, 1961.

5. Beard, David B.: The Interaction of the Terrestrial Magnetic Field with the Solar Corpuscular Radiation. J. Geophys. Research, vol. 65, no. 11, Nov. 1960, pp. 3559-3568.

6. Kawashima, Nobuki: The Interaction of a Plasma Stream with a Three-Dimensional Dipole. Phys. Soc. Japan J., vol. 19, no. 2, Feb. 1964, pp. 227-234.

7. Odishaw, Hugh, ed.: Sun, Upper Atmosphere and Space. Vol. 1 of Research in Geophysics. MIT Press, 1964, p. 184.

8. Levy, Richard H.: Radiation Shielding of Space Vehicles by Means of Superconducting Coils. Res. Rep. No. 106, AVCO Everett Research Lab. April 1961.

9. Shkarofsky, I. D.: The Solar Wind, the Magnetosphere and their Simulation in the Laboratory, Res. Rep. No. 7-801, RCA Victor Co, Ltd., Montreal, Canada, Oct. 22, 1962.

10. Tsu, T. C.: Interplanetary Travel by Solar Sail. ARS J., vol. 29, no. 6, June 1959, pp. 422-427.

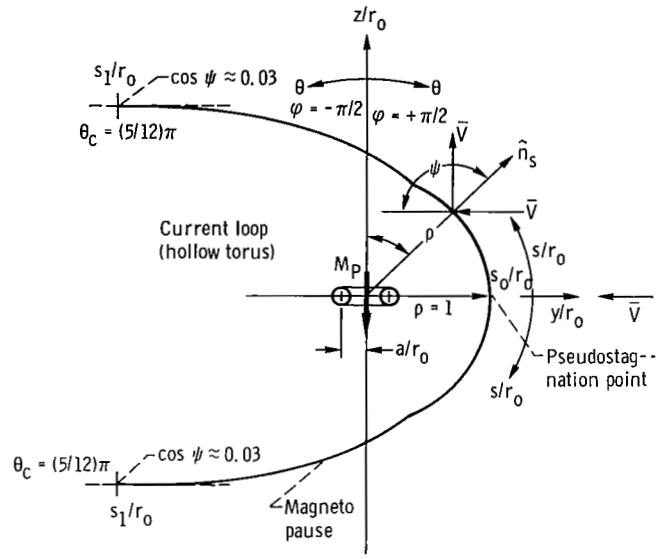

Figure 1. - Three-dimensional magnetosphere showing cross-sectional view in meridian plane at zero degree angle of incidence.

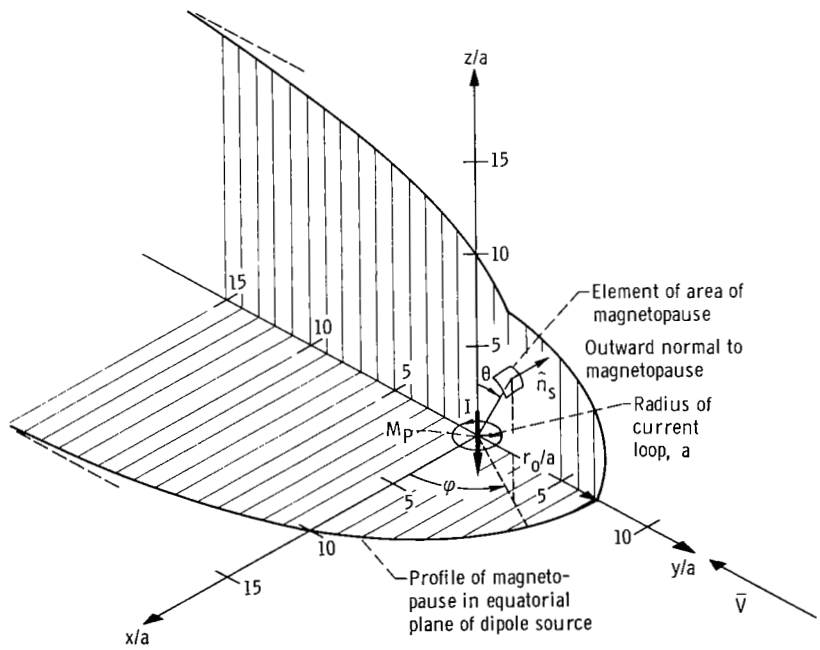

Figure 2. - View of coordinate system and boundary of equatorial plane and meridian plane containing current loop axis and Sun-Earth line at zero degree angle of incidence.

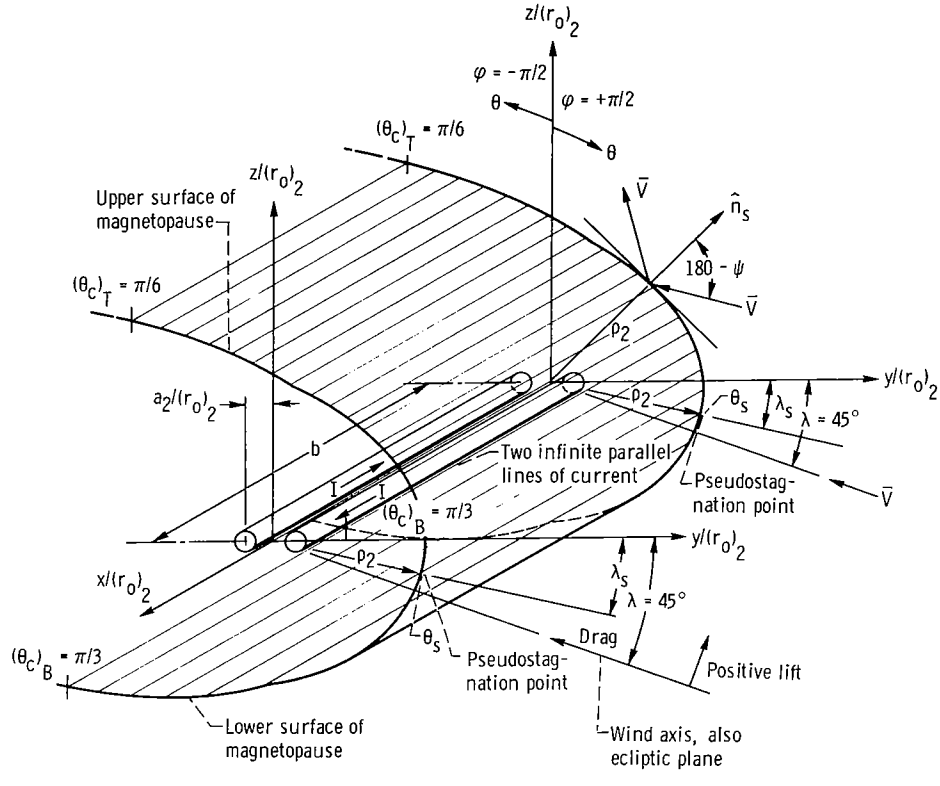

Figure 3. - Segment of two-dimensional magnetosphere at zero degree angle of incidence.

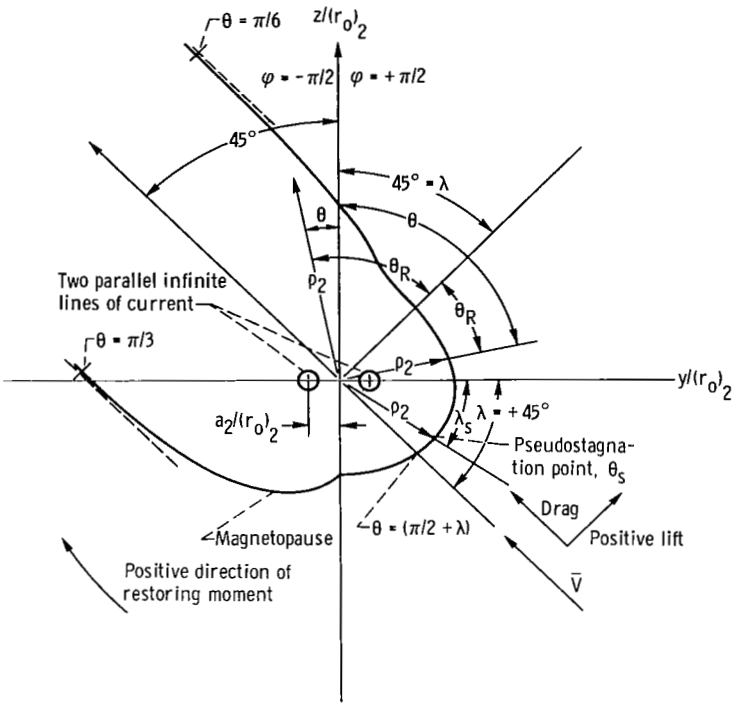

Figure 4. - Cross-sectional view showing meridian plane and moment center for two-dimensional case at 45° angle of incidence.

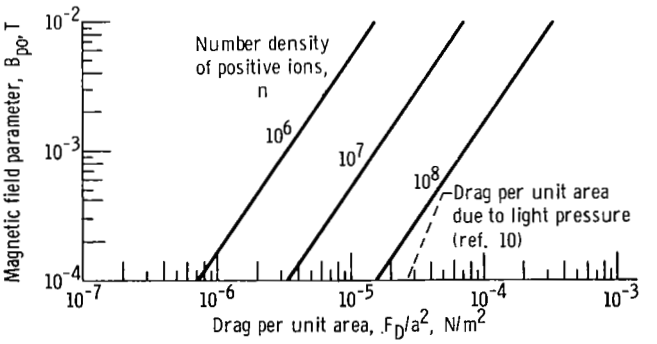

Figure 5. - Magnetic field parameter plotted against ratio of drag to current-loop radius at zero degree angle of incidence for current loop.

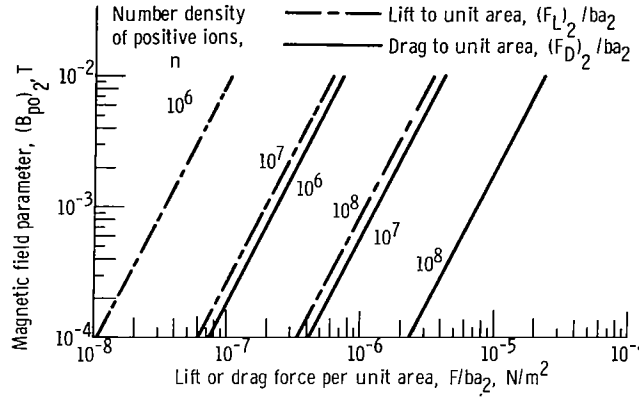

Figure 6. - Magnetic field parameter plotted against ratios of lift and drag per unit area per unit length of span at 45^0 angle of incidence for two parallel infinite lines of current.

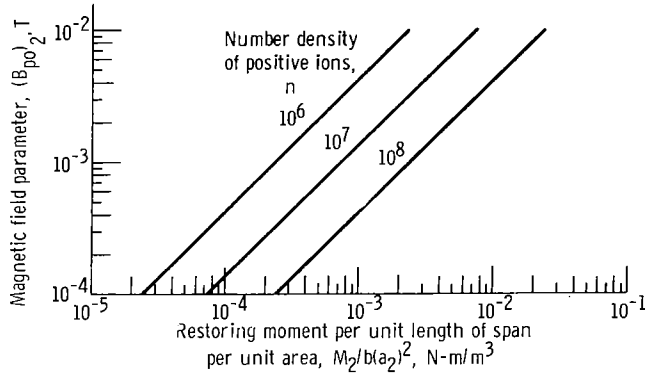

Figure 7. - Magnetic field parameter plotted against restoring moment per unit area per unit length of span at 45^0 angle of incidence for two parallel infinite lines of current.

NASA-Langley, 1968 — 28 E-3253